Global NEST Journal, Vol 25, No 10, pp 33-46

Biosorption of heavy metals using *Gracilaria edulis* seaweed – batch adsorption, kinetics and thermodynamic studies

Gopalakrishnan Preethi[1]* and Jeyadharmarajan Jeyanthi[2]
[1]Department of Civil Engineering, Sri Krishna College of Engineering and Technology, Coimbatore, Tamil Nadu, India
[2]Department of Civil Engineering, Government College of Technology, Coimbatore, Tamil Nadu, India
Received: 26/07/2023, Accepted: 25/09/2023, Available online: 06/10/2023
*to whom all correspondence should be addressed: e-mail: g.preethi6392@gmail.com
https://doi.org/10.30955/gnj.005259

Graphical abstract

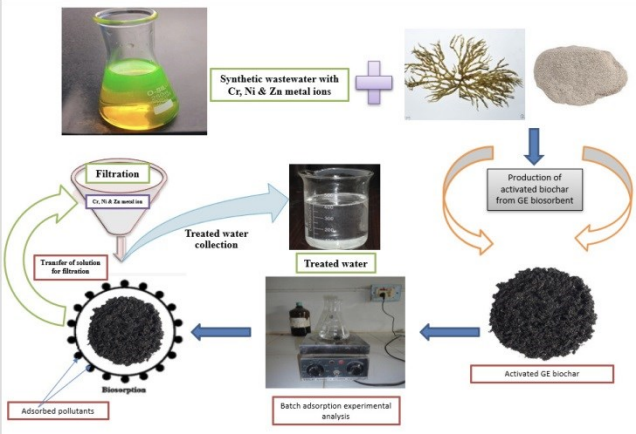

Abstract

Clean water and its requirement are one of the emerging needs in recent days. Water pollution creates more amount of toxic nature to the clean water and it increases the accumulation of poisonous contaminants in the water sources. Heavy metal ions are the type of toxic pollutant released from textile industrial effluent, changes the natural color of clean water. In this study, Adsorption behavior with activated biochar Gracilaria edulis as adsorbent was investigated under batch mode for removing detecting elevated levels of metallic cations in aqueous solutions. The biochar adsorbent was prepared with chemical synthesis process and their surface area analyzed using N_2 adsorption process. The presence of targeted heavy metal ions was confirmed using SEM and EDX analysis. The maximum adsorption efficiency of 99.9% of Cr, 97.37% of Ni and 92.73% of Zn heavy metal ions was achieved using the biochar adsorbent. The endothermic reaction in between adsorbent and adsorbent was confirmed using the thermodynamic studies and maximum amount of spent adsorbent was recovered by using desorption process by adding strong hydrochloric acid with 0.3 N.

Keywords: Biosorption, *Gracilaria edulis,* batch studies, kinetics and thermodynamics, desorption

1. Introduction

Water pollution is one among the serious threat faced by most of the developing nations. The physical and chemical characteristics of water gets drastic changes due to rapid applications of chemicals and toxic minerals through industrial activities. The changes of the characteristics may cause a serious health issue to the surrounding environment due to the toxic substance (Priya et al, 2022). Clean water is required for all living beings around the globe for the survival. Nowadays the quality of water getting reduced due to the presence of toxic pollutants along with organic and inorganic pathogens. These pollutants are non-degradable which creates dangerous effects even in very low concentration level. There are lot of toxic pollutants such as heavy metals, heavy metal ions, microbes, fertilizer and pesticides etc. released from various industrial and manmade activities which are mixed with the natural water resources (Eleryan et al, 2022). Among all the pollutants, chemical heavy metal ions play a vital role to create the high amount of toxicity in water. Excess amount of industrial wastewater with or without treatment release into natural water bodies which creates depreciation of water quality around the world. Apart from the organic pollutants, heavy metals and heavy metal ions are non-degradable produced the harmful end product. The heavy metal ion pollution existing in the aqueous waste from textile industries may create aqueous toxicity and converts natural water into most poisonous state (Pham et al, 2021).

To eliminate the contamination caused by metal cations in the aqueous solutions is one of the major challenging tasks and it needs very high capital investment. Membrane separation, adsorption, chemical precipitation, coagulation & flocculation, and ion-exchange are the common treatment methods which are used widely for purging heavy metal cation contaminations from the aqueous medium. These methods were not utilized properly in real time experimental works due to secondary sludge generation, usage of harmful chemicals, skilled person requirement and high-cost investment (Fideles et al, 2019). In recent days, there is an urgent

need to develop an innovative treatment methodology with very low capital and investment cost. Among these methods, the adsorption process is one of the treatment techniques which has been used in recent days for removing pollutants from aqueous solutions. This method requires very low investment and there is no secondary sludge formation during the wastewater treatment (Boubaker et al, 2021). The development of adsorption is based on the efficiency of the adsorbent material. The accumulation of pollutants atop the adsorbent surface material due to wan-der walls force and its attraction is called adsorption process. There are numerous eco-friendly and artificial materials employed as an adsorbent material to take in the toxins from the wastewater (Khan et al, 2022). Various types of heavy metal ions (Cr, Ni and Zn etc.) are available based on the type of industrial activities and the adsorbent material may provide very high amount of efficiency rate for a selective heavy metal ion removal. Selecting the adsorbent material is important for adsorption process to have a better removal rate. In this study, the activated biochar *Gracilaria edulis* charcoal was used as an adsorptive material for removing the Cr, Ni and Zn heavy metal ions from the synthetic solutions. The heavy metal ions of Cr, Ni and Zn are common heavy metal ions available in various textile industrial effluents may create aquatic toxicity and poisonous effects on the atmosphere.

In this investigation, Gracilaria edulis was employed as a sorbent material for extracting heavy metal cations from synthetic solutions. using batch adsorption technique. Gracilaria edulis, a red seaweed commonly known as sea moss or agar weed, exhibits several key characteristics that make it valuable in water treatment applications. Its ability to absorb and take up nutrients, particularly nitrogen and phosphorus, is beneficial in reducing excessive nutrient levels and combating harmful algal blooms (Venkataraghavan, et al, 2020). The branching structure of Gracilaria edulis allows it to act as an effective filter, removing suspended solids, organic matter, and particulate pollutants from the water, leading to improved clarity and reduced turbidity. Moreover, the seaweed demonstrates the capacity to absorb heavy metals, making it valuable in treating industrial wastewater and polluted water bodies. Through photosynthesis, Gracilaria edulis releases oxygen into the water, promoting aerobic conditions and supporting aquatic life. Additionally, its presence can inhibit the growth of harmful algae, contributing to better water quality (Isam et al, 2023). Its fast growth rate and ability to be cultivated in large quantities enable efficient biomass production for various applications in water treatment. While these characteristics make Gracilaria edulis promising for water treatment, the effectiveness of its implementation may vary based on environmental factors and specific treatment goals. Hence, it is decided to use *Gracilaria edulis* as adsorbent material to remove the Cr, Ni and Zn heavy metal ions from the synthetic solutions. The biochar derived from the *Gracilaria edulis* was used in this study and the influence of heavy metal ion elimination was examined under diverse operational parameters in a batch adsorption process.

2. Materials used and methods

2.1. Gracilaria edulis collection

Gracilaria edulis, also known as sea moss or agar weed, is typically found in coastal areas and marine environments. It can be collected from rocky shores, intertidal zones, and shallow subtidal regions where it thrives attached to rocks, substrates, or other seaweed species. Gracilaria edulis is commonly distributed in regions with moderate to warm climates, such as tropical and subtropical areas. For collecting any seaweed (including Gracilaria edulis), it's essential to ensure that you have the necessary permits or permissions for harvesting seaweed in these areas. Additionally, it's crucial to follow sustainable harvesting practices and avoid overexploitation to protect the natural marine ecosystem. Rameswaram and Thoothukudi (Tuticorin) are coastal areas in Tamil Nadu, India, where Gracilaria edulis is collected. Rameswaram, situated at approximately 9.2870° N latitude and 79.3129° E longitude, offers a favorable environment for the growth of this seaweed species. Thoothukudi, located at around 8.7642° N latitude and 78.1347° E longitude, is another potential collection site for Gracilaria edulis. These regions are known for their coastal biodiversity and proximity to the Gulf of Mannar and Palk Bay, which are favorable habitats for various seaweed species.

2.2. Activated Gracilaria edulis biochar preparation

The *Gracilaria edulis (GE)* collected from various areas in and around Rameswaram and Thoothukudi is washed and dried under sun. After 24 hours of sun drying process, they were collected and cut into small pieces and allowed for continuous grinding. In a closed vessel, 10g of GE and 10mg of citric acid (used as a carbonization catalyst) were treated to hydrothermal carbonization for five hours at a maximum temperature of 225 degrees Celsius. Using the double distilled water, the GE biochar was washed thoroughly and dehydrated in an oven set at 176°F for Half a day. To increase the surface area of the prepared hydro charcoal adsorbent, the hydrogen peroxide (H_2O_2) solution was used. The prepared hydro charcoal powder was immersed into the H_2O_2 solution for a period of 24 hours and placed in an oven for further heating. Then the sample was collected and washed several times with distilled water and used for further experimental works. To prepare the synthetic solution with heavy metal ions, the chemicals containing Cr, Ni and Zn were used. The cleansing process for these heavy metal ions are not required since it is of analytical grade and these are all widely used in all types of textile manufacturing industries. The double distilled water 1000 ml capacity was added with these heavy metal ions and used as synthetic solution for the entire experimental works.

2.3. Characterization of biochar adsorbent

By nitrogen adsorption at -196°C, the area of adsorbent specific surface and the structure of pore were identified using surface area analyzer. The sample was kept at 300°C

for a period of 3 hrs to remove gas or vacuum and surface area (S_{BET}) of Gracilaria edulis charcoal powder estimated by Brunauer Emmett Teller (BET) analysis. The micropore (S_u) and meso pore (S_m) area of the surface obtained by employing the Dubinin-Radushkevich (D-R) method, utilizing the equation $S_m = S_{BET} - S_u$. Under significantly elevated pressure (P/Po ≈ 0.99) utilizing a liquid nitrogen volume, total volume of the pore (V_T) was calculated. The micro and meso pore volumes (V_u and V_m) of sample were derived using the relationship $V_m = V_T – V_u$. The equation $DP = 4VT/S_{BET}$ is utilized within the Barrett Joyner Halenda (BJH) model for determining both the pore distribution of activated carbon powder and the mean pore diameter (D_P). The functional groups and chemical characteristics present in the prepared Gracilaria edulis charcoal powder was identified by Fourier Transform Infrared Spectroscopy (FTIR) analysis. A solution with a pH of 6 was created by combining 25 mg/L of concentrated synthetic solutions containing specific metal ions with 1 gram of Gracilaria edulis charcoal powder adsorbent. The mixture was placed inside a rotary shaker and subjected to shaking at a speed of 200 revolutions per minute (rpm) for a duration of approximately 3 hours. The suspension was then left undisturbed in the flask. Following a designated period, the suspension was retrieved from the flask and employed for subsequent experimental analyses. To perform FTIR analysis, the scanning range of 400 - 4000 cm^{-1} was established with a resolution of 4 cm^{-1}. The spectra of the adsorbent sample were generated by conducting up to 20 scans prior to and following the absorption of metallic cations. To verify the existence of the specific metal ions on the surface of the adsorbent, Scanning Electron Microscopy (SEM) coupled with Energy Dispersive X-Ray (EDX) analysis was performed. The examination was conducted using a 10 kV voltage level and a working distance of 15 µm, employing SEM and EDX analysis to ascertain the elemental and physical characteristics of the adsorbent. Furthermore, X-ray Diffraction (XRD) analysis was performed to evaluate the crystalline structure of activated sawdust charcoal powder. This analysis involved using CuK-α radiation with a power of 40 kV and a current of 250 mA, and various peaks were examined during the XRD analysis.

2.4. Batch adsorption studies

The operating conditions for adsorption process under batch mode using activated GE biochar was adjusted by various intervals. The batch studies performed by adjusting the parameters pH, time of contact in between the heavy metal ions and biochar Gracilaria edulis adsorbent, Biochar carbon dosage, concentrations of metal ions, and the temperature of heavy metal ions were all carefully prepared for the experiment. The pH level of heavy metal ions in synthetic solution was adjusted from 2.0 to 7.0 by adding buffer tablets and the temperature of the solution was maintained at 30°C with 1 hr. of equilibrium time. During the initial stage of batch adsorption study, metal ion concentrations were fixed at 60mg per L in 100 mL aqueous solution. To identify the optimum level of Gracilaria edulis biochar carbon dosage, the amount of adsorbent was varied from 0.5 to 2.5 g/L and poured into the known concentration of heavy metal ions. The duration of contact between the Gracilaria edulis adsorbent and the solution containing metallic cations was adjusted within the range of 15 to 120 minutes. To attain the equilibrium, the solution was kept in shaker and allowed for continuous stirring for a period of 1 hour. Equation 1 used to find out the amount of heavy metal ions uptake by activated biochar Gracilaria edulis adsorbent during the equilibrium time.

$$q_t = \frac{V}{M}(X_o - X_t) \quad (1)$$

Amount of metal ions adsorbed by the GE biosorbent was evaluated using q_t in mg/g, the concentration of metal ions for this batch study was represented by X_t. The volume and volume of batch study was represented by v and m. Following an equilibrium time of 1 hour, the solution was subjected to an additional 5 minutes of centrifugation in the shaker. The resulting suspension was then retrieved, and the concentration of heavy metal ions was determined using Spectroscopy (AAS). To get the concurrent value, each analysis made 2 trials. Equation 2 used to express the mass balance approach of the adsorption system.

$$\% \text{ Removal} = \left[\frac{X_o - X_e}{Xo}\right] X100 \quad (2)$$

The initial and concluding concentration of heavy metal ions in synthetic solutions during the equilibrium time represented by X_o and X_e in mg/L.

2.5. Adsorption isotherm studies

The isothermal studies with various analysis were used to check the adsorbate transmission from the phase of solution to the phase of adsorbent in the condition of equilibrium (Fakhar et al, 2021). The adsorbate molecules and its interaction with the active sites of adsorption was described by using the isotherm studies. In this study, six isothermal analyses were made to know the behavior of adsorption process using GE biosorbent.

2.5.1. Langmuir isotherm study

This study was employed to illustrate the equilibrium established among the adsorbent and gaseous phases. Through this isotherm, the correlation between the concentrations of the solid adsorbent and the fluid was established, facilitating a comprehensive understanding of the alterations taking place during the adsorption process (Kaminski et al, 2015). It serves as a valuable means of comprehending the adsorption behavior and defining the equilibrium state between the two phases. The isotherm study process entails monolayer adsorption occurring on the surface of the adsorbent under varying relative pressures and heterogeneous conditions (Khan et al, 2020). Through chemical reactions, binding mechanism was happened in between adsorbent and adsorbate. The linear relationship among adsorbent and adsorbate uptake has been expressed using the equation 3 by Langmuir model.

$$\frac{C_e}{q_e} = \frac{1}{K.q_{max}} + \frac{C_e}{q_{max}} \quad (3)$$

Where, C_e – Solution's concentration at the equilibrium in mg/L, q_e – Adsorbed amount of metal ions per gram, K & q_{max} – Constants of Langmuir isotherm equation related to capacity and intensity of adsorption.

2.5.2. Freundlich isotherm study

Through the application of this study, the alterations in the quantity of gas adsorbed per unit mass of adsorbent were investigated by modifying the system pressure at a specific temperature. This thermodynamic analysis allows for the formation of several layers of adsorption scheduled the surface of the adsorbent (Su et al, 2021). Based on the heterogeneous surface adsorption this isotherm model was developed. The linear relationship between adsorbent and adsorbate uptake has been expressed using the equation 4 by Freundlich model.

$$\frac{C_e}{q_e} = \frac{1}{q_m K_e} + \frac{C_e}{q_m} \quad (4)$$

Where, q_e – Adsorbed quantity of adsorbate per gm and K_e – Capacity of adsorption related to Freundlich constant

2.5.3. Sips isothermal study

Both Langmuir and Freundlich isotherm models were combined together to analyze the heterogeneous nature of adsorption process and its prediction within the limiting behavior using the sips isotherm studies (Obulapuram et al, 2021). Also, the concentrations of the adsorbate were neglected. Therefore, it conforms to the monolayer adsorption mechanism. The mathematical representation of Sips model linear study has been expressed in Equation 5.

$$\frac{1}{q_e} = \frac{1}{Q_{max} K_s \left(\frac{1}{C_e}\right)^{\frac{1}{n}}} + \frac{1}{Q_{max}} \quad (5)$$

Where, Q_{max} and Ks represent the adsorptive capability and equilibrium coefficient, respectively, and are derived from the gradient and y-intercept of the linear plots. The factor of heterogeneity, denoted by 'n,' ranges between 0 and 1.

2.5.4. Toth isothermal study

This isothermal model was developed to address the discrepancies that Langmuir isotherm model. It aims to minimize the disparities and improve the accuracy of the model by considering additional parameters or factors that may influence the adsorption process. The Toth isotherm study elucidates the adsorption process at both very low and high concentrations of heavy metal ions (Konicki et al, 2017). The mathematical representation of Toth isothermal model was represented in Equation 6. This model is designed to capture the behavior of adsorption over a wide range of concentrations and provides valuable insights into the adsorption phenomenon.

The linear equation for the model is given by equation 6.

$$\ln \frac{q_e}{q_m - q_e} = n \ln K_L + n \ln C_e \quad (6)$$

The isotherm constants were represented by K_L and n and adsorbed materials and its quantity was represented by q_e.

2.6. Adsorption kinetic studies

2.6.1. Pseudo first order

This kinetic model also called as Lagergren kinetic model used to establish the solid adsorption capacity with liquid and solid systems. The speed at which metallic cations desorbs is directly correlated with the driving force, which serves as the fundamental presumption of this kinetic model (Yogeshwaran et al, 2021). The variations between initial and equilibrium concentrations ($q - q_e$) has been assessed using the metal ion adsorption using GE biosorbent. The mathematical representation of this kinetic model was represented in Equation 7.

$$\frac{dq_e}{dq_t} = k\,(q_e - q_t) \quad (7)$$

Equation 7 is rearranged to equation 8 by applying the boundary conditions to find out q_e and q_t values.

$$\log(q_e - q) = \log q_e - \frac{k}{2.303} t \quad (8)$$

2.6.2. Pseudo second order

The second order kinetic model was used under the basic assumption of the rate of adsorption is directly proportional to the availability of empty sites in the biochar adsorbent. The mathematical representation of this kinetic model was represented in Equation 9.

$$\frac{t}{q_t} = \frac{1}{k q_e^{\,2}} + \frac{t}{q_e} \quad (9)$$

The adsorption rate during initial time was represented by kq_e^2 and the adsorbent rate constant was represented by k.

2.6.3. Boyd kinetic study

The determination of the rate-controlling step for heavy metal adsorption by the biosorbent involved the application of the Boyd kinetic model. Equation 10, known as the Boyd kinetic equation, was utilized for data analysis. Once the B values from the Boyd kinetic plots were obtained, Equation 11 was employed to calculate the effective diffusion coefficient (Di).

$$Bt = -0.4977 - \ln(1 - F) \quad (10)$$

$$B = \frac{\Pi^2 D_i}{r^2} \quad (11)$$

2.6.4. Elovich kinetic study

The evaluation of the biochar adsorbent and its interaction with gas molecules during the initial stages of heavy metal ion acceptance involved the utilization of this kinetic study (Singh et al, 2018). This kinetic model assumes an exponential increase in the desorption rate as the adsorbed solute decreases, and vice versa. Equation 12 represents the linear equation that represents this Elovich kinetic model.

$$q_t = \frac{1}{b} \ln(1 + abt) \quad (12)$$

The parameters "a" and "b" represent the ability of adsorption and the constant for desorption, respectively.

3. Results and discussion

3.1. BET surface area analysis

The BET isotherm plot is shown in Figure 1 and the linear plot represents the adsorbed volume of N_2 is properly fitted with the relative pressure. The isotherm curve represents that the adsorption process is classified as type-I, indicating the presence of micro or mesopores were observed in the prepared biochar activated adsorbent (Sheeja et al, 2021). The activated biochar Gracilaria edulis adsorbent has very high surface area of 96.585 m^2 g^{-1} other than the activated carbons that are commercially available with the pore volume of 0.9740 cm^3 g^{-1} and pore radius of 11.821 Å. The comparison between biochar and biochar activated *Gracilaria edulis* adsorbent was represented in Table 1.

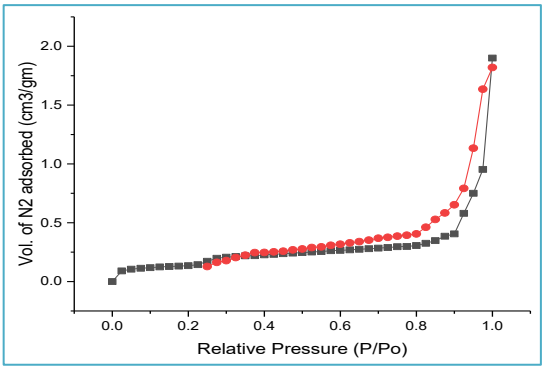

Figure 1. BET surface area analysis of GE biochar by nitrogen

Table 1. Raw and Activated GE biochar characteristics in BET surface analysis

S. No.	Parameter	GE - Raw Adsorbent	GE - Biochar Adsorbent
1.	BET surface area	57.747 m^2/g	96.585 m^2/g
2.	Volume of Pore	0.094 cm^3/g	0.9740 cm^3/g
3.	Volume of Pore (Micro)	0.189 cm^3/g	0.236 cm^3/g
4.	Volume of Pore (Meso)	0.082 cm^3/g	0.112 cm^3/g
5.	Area of Pore (Micro)	392 m^2/g	438 m^2/g
6.	Radius of Pore (Avg.)	14.881 Å	11.821 Å

3.2. SEM analysis

The Microscopic analysis of raw *Gracilaria edulis* powder, biochar and activated biochar *Gracilaria edulis* charcoal powder after adsorbing the metallic cations of Cr, Ni and Zn was shown in Figure 2a and 2b respectively. By referring the SEM image of raw adsorbent powder (Figure 2a), the availability of active sites is very low. The active sites were used to receive the pollutants on the top side of GE biosorbent's surface. Figure 2b shows the SEM image of biochar powder before activation process and Figure 2c shows the activated biochar adsorbent material's SEM image. With the outcome of these figures, availability of active sites and surface area are very high in activated biochar *Gracilaria edulis* adsorbent material. With respect to Figure 2c, it was clear that an uneven pores on the top of biochar activated adsorbent which may use to receive the pollutants from the sources. The pores were created through the chemical activation using hydrogen peroxide, and they play a crucial role in attracting pollutants from the aqueous medium. These pores serve as highly beneficial structures for the adsorption of pollutants and help in effectively removing them from the water (Marciniak et al, 2022). Figure 2d displays the SEM images of the GE biochar following the adsorption process of heavy metal ions. The images provide visual insights into the morphological changes and potential interactions between the adsorbent and the adsorbed heavy metal ions. The biochar-activated Gracilaria edulis adsorbent material exhibits a remarkably high capacity for adsorbing pollutants from aqueous solutions. This indicates its strong affinity and effectiveness in effectively capturing and removing pollutants present in the water (Nippes et al, 2022). The surface of biochar activated adsorbent was completely filled with pollutants, the activated carbon forms a cloud-like layer on the upper surface (Figure 2d). There are empty sites remaining on GE biochar surface indicates the accomplishment of adsorption process. Also, the synthetic heavy metal ions react and undergo protonation without causing any damage to the existing functional groups present in the adsorbent. The amount of targeted heavy metal ions adsorption and the behavior of adsorbent material were evaluated by the following EDX analysis.

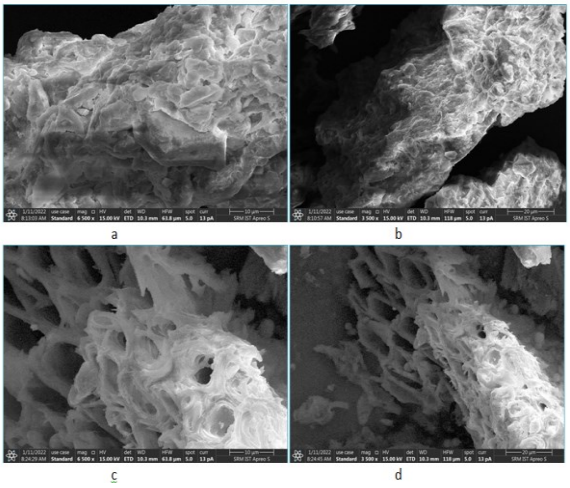

Figure 2. SEM images of (a) GE Raw powder, (b) GE Biochar charcoal, (c) GE Biochar with chemical activation & (d) GE Activated biochar after the adsorption of heavy metal ions respectively

3.3. EDX analysis

This analysis was conducted individually to evaluate the presence of targeted heavy metal ions from the synthetic solutions under various conditions. Figure 3(a) and 3(b) depict the EDX image of the raw Gracilaria edulis adsorbent, revealing the presence of both organic and inorganic elements. The prepared adsorbent material underwent activation with hydrogen peroxide after the biochar preparation, as shown in the mentioned figure. Referring to the EDX image (Figure 3b) it was observed the occurrence of targeted metal ions along with other elements such as magnesium, calcium and oxygen etc. The synthetic solutions containing the heavy metal ions were passed into the activated biochar adsorbent and the amount of heavy metal ions uptake by the biochar

adsorbent was examined. The EDX analysis revealed the presence of various other natural and synthetic materials, including constituents such as Mg, Si, Fe, and more.

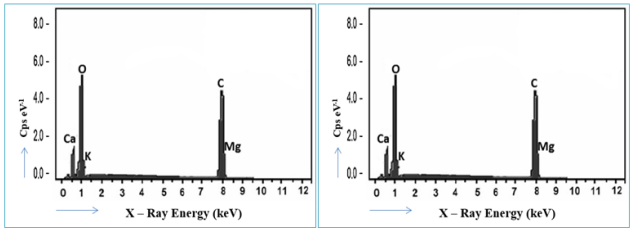

Figure 3. (a) EDX image of GE before metal ion adsorption and 3 (b) EDX image of GE after-metal ion adsorption

3.4. FTIR analysis

The FTIR functional groups were identified for raw, biochar and activated biochar adsorbent and shown in Figure 4a & b. Based on the bandwidth in energy regions the adsorbent displays a variety of distinct functional groups was analyzed to make the adsorption process in effective manner. The FTIR image reveals a pronounced energy region with band widths of 3420 cm^{-1} and 2860 cm^{-1}, suggesting the presence of functional groups like hydroxyl (-OH) and methylene ($-CH_2$) moieties (Chakraborty et al, 2022). The presence of various elements such as water at 1670 cm^{-1}, aromatic vibrations in between 1600 – 1400 cm^{-1}, $-CH_2$ bending at 1400 – 1380 $cm^{-1}$and C-O vibrations at 1090 cm^{-1} was observed within the range of 1900 – 1200 cm^{-1}. The bending of -C-H bonds attributed to aromatic vibrations was observed at a band width of 1000 cm^{-1}. Due to vibrations by aromatic ring, -OH stretching was developed in lower frequency regions and the $-CH_2$ stretching vibrations was extinct at the band level of 2860 cm^{-1}. FTIR studies have confirmed the presence of diverse natural and synthetic functional groups in the activated biochar Gracilaria edulis adsorbent material. Furthermore, these studies confirm its ability to adsorb pollutants from aqueous media during the adsorption process.

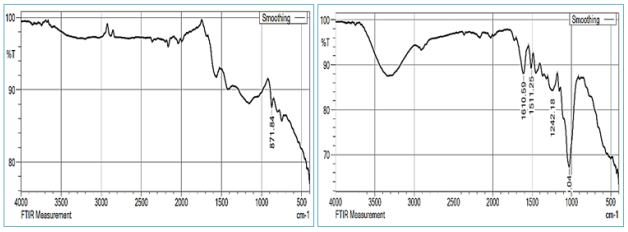

Figure 4. (a) FTIR image of GE before metal ion adsorption and 4 (b) FTIR image of GE after-metal ion adsorption

3.5. XRD analysis

Figure 5a and 5b illustrate the XRD peaks corresponding to the untreated biochar and the activated biochar (Gracilaria edulis adsorbent), respectively. The unprocessed adsorbent has very low crystalline structure and intensity when compared to the activated biochar adsorbent by referring the XRD figures. The activated biochar adsorbent seems to be good in compare with the XRD peaks at 150, 230, 270, 301, 385 and 470 at 25 matches with 90, 120, 70, 50, 45 and 30 hkl planes respectively. The crystalline structure was very helpful for the adsorbent to hold the received contaminants in the aqueous solution. The activated biochar adsorbent has very high crystalline structure than raw adsorbent (Yan et al, 2020). Also, intensity is very high in activated biochar adsorbent which introduces the diffractions and higher pitching.

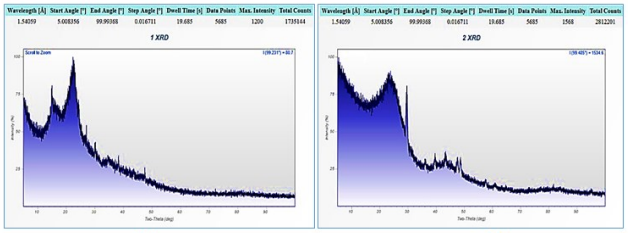

Figure 5. XRD peaks of GE biosorbent (a) before and (b) after the chemical activation process

3.6. Impact of pH in heavy metal ions removal

Batch adsorption study, with varying the pH values from 2.0 to 7.0 by fixing the heavy metal ions concentration, biochar adsorbent dose, contact time and temperature from which the impact of heavy metal ions uptake is evaluated. The decrease in pH of heavy metal ions solution may increases the heavy metal ions uptake by activated biochar adsorbent was witnessed by referring the Figure 6a. The adsorbents with a negative charge on their surface increase the interaction between heavy metal ions and activated biochar Gracilaria edulis adsorbent. The high positive charge was developed by the adsorbent during the very high pH level which attributes faster removal of heavy metal ions (Aguilar et al, 2022). At pH 2.0, maximum amount of targeted heavy metal ions adsorbed the biochar adsorbent. When pH is high, hydroxide precipitation was attributed which reduces the heavy metal ions uptake by the biochar adsorbent. From this study, the activated biochar adsorbent takes 99.9% Cr, 97.37% Ni and 92.73% Zn heavy metal ions from the synthetic solution at the optimum pH of 2.0.

3.7. Impact of biochar dose in heavy metal ion removal

The analysis focused on the effect of metal ion adsorption using GE while varying the activated biochar dose from 0.5 - 2.5 mg/L, while keeping the pH, contact time, heavy metal ions concentration, and temperature constant. The decrease in concentration of adsorbent dose may decreases heavy metal ions uptake from synthetic solutions. In Figure 6b, the consequence of targeted pollutants uptake is depicted by altering the concentration of activated biochar and it was observed the gradual decrement in heavy metal ion adsorption when the adsorbent dose was decreased. The energetic locations and its accessibility are very low in lower dosage levels which may reduce the heavy metal ions uptake from the aqueous solutions (Xi et al, 2020). At an optimum GE biochar dosage of 2 mg/L, 98.73% of Cr, 87.92% of Ni & 79.26% of Zn grade heavy metal ions was achieved by the adsorbent and beyond 2 g L^{-1}, the heavy metal ions uptake was stabilized due to the concentration gradient decrement. Due to the availability of free surface

at the time of heavy metal ions uptake by the biochar may developed the concentration gradient.

3.8. Impact of contact time in heavy metal ion removal

The interaction in between adsorbent and pollutants are affected by the contact time during the adsorption process. There was a ten-minute to one-hour contact time with the biochar adsorbent between heavy metal ions and the concentrations of each heavy metal ion attuned from 25 - 150 mg/L. During the initial stages, due to the high availability of active sites in the activated biochar adsorbent, heavy metal ions uptake by the activated biochar adsorbent was very high as shown in Figure 6 c, d, & e. Due to the low vacant sites and force of repulsion acting on the surfaces of the adsorbent molecules after 50 minutes, the removal of heavy metal ions from the aqueous solutions reached saturation. Also, the heavy metal ion molecules need very high strength to travel into the biochar adsorbent pores may reduce the heavy metal ions uptake during the final stages. Finally, the heavy metal ions uptake was reached the constant rate (Haro et al, 2021).

3.9. Influence of heavy metal ions concentration in adsorption

Heavy metal ions concentrations were adjusted from 25 to 150 mg/L with a pH 2.0 heavy metal ions solution and 2 mg/L biochar adsorbent dosage, and the impact of heavy metal uptake using the biochar was evaluated. In Figure 6f, it can be observed at the initial phase when the concentration of heavy metallic cations is low, the biochar adsorbent exhibits a high uptake of heavy metal ions due to the presence of numerous active sites on its surface. However, as the concentration of heavy metal ion solutions increases, there is a sharp decrease in the uptake. The mesopores of the adsorbent reach their capacity as they become saturated with the adsorbed heavy metal ions. The biochar activated Gracilaria edulis powder adsorbed 99.75% Cr, 94.65% Ni, and 89.82% Zn category heavy metal ions in very low concentrations. The quick assimilation of heavy metal ions by the adsorbent at lower concentrations indicates that the biochar adsorbent was not overloaded, as it effectively captured the ions (Alardhi et al, 2020).

3.10. Isotherm studies

3.10.1. Langmuir isotherm

The Langmuir isotherm study is illustrated in Figure 7a, which shows the linear relationship between C_e/q_e and Ce. To obtain the slope and intercept from each plots the values of the constants of Langmuir isotherm, namely k and q_{max}, were determined. Table 2 shows, coefficient of regression values achieved from Langmuir kinetic plots at 30°C temperature. Using 25 mg/L heavy metal ion concentrations, the separation parameters of Cr, Ni, and Zn cadre heavy metal ions were 0.0039, 0.0184, and 0.0314, respectively. The values are lied between 0 to 1 may confirm the process of heavy metal ions adsorption was excellent condition (Krishna Murthy et al, 2020).

3.10.2. Freundlich isotherm

Figure 7b display the linear graphs of this study, depicting the relationship between ln q_e and ln C_e and those plots were used to obtain the constants of this model, K_f and n. Referring the Table 2, the coefficient of regression values was obtained from Freundlich kinetic plots at 30°C temperature. The n values of 3.580 for Cr, 2.986 for Ni and 2.658 for Zn are lies in between 1 to 10 may verify the development of heavy metal adsorption follows physical nature (Venkatraman et al, 2021). The experimental data found after the Langmuir and Freundlich plots are properly correlated with the regression values (R^2) and it shows the evidence of applicability of this model and physical adsorption process.

3.10.3. Sips isotherm

Figure 7c illustrates the linear plots of this model, showcasing the relationship between the equilibrium data and the model. The corresponding model constants derived from each plot are presented in Table 2. The n value (Heterogeneity factor) from each plot was calculated and it will be useful to find out the nature of the adsorption process, distinguishing between heterogeneous and homogeneous adsorption (Benjelloun et al, 2021). The obtained regression values (R^2), which are greater than 0.95, strongly support the suitability and applicability of the Sips isotherm study, indicating a robust fit among the data obtained from the model and experimental analysis. The n value ranging between 0 and 1 indicates a possible fitting with either the Langmuir or Freundlich isotherm models. When 'n' is equal to 1, it signifies that the adsorption process follows the Langmuir isotherm model.

3.10.4. Toth isotherm

The heterogeneous solid surface was identified by using the Toth isotherm study and its constant values. Figure 7d depicts the linear plots this study, providing visual representation of the relationship between the equilibrium data and the model. The corresponding model constants, including Qmax, bT, and nT, are presented in Table 2. Three constants were derived from the linear plots and this model is usually called as three-parameter model provides very high accuracy of isotherm fitting (Wang et al, 2022). The interaction between the biochar adsorbent surfaces and heavy metal ions pollutants were analyzed in this model and the regression value (R^2) of each plot were lower than 0.95 and it does not fit with the adsorption process. When the Langmuir isotherm data exhibited a satisfactory fit with the equilibrium data, the Toth isotherm linear plots were employed to establish a connection between the equilibrium and the adsorption process of heavy metal ions using the biochar adsorbent. But the Langmuir data was fitted well in this adsorption process and Toth isotherm study is not necessary to check the favorable fitting of adsorption process.

3.11. Kinetic studies

3.11.1. Pseudo first order kinetic study

The adsorption kinetics are described by the Pseudo first order studies by plotting the kinetic plots of [(q_e – q) vs. t]. Figure 8 (a), (b), (c), shows the kinetic plots of Pseudo first order studies for Cr, Ni and Zn heavy metal ions uptake by the activated biochar *Gracilaria edulis* adsorbent. The

kinetic model constant (k) was derived by adjusting the heavy metal ions concentrations of metal ions and the regression values (R^2) were calculated from each plot and represented in Table 3. All the regression values calculated from each plot were in good agreement with the metal ion adsorption process and high regression (> 0.95). The significance of this kinetic model lies in its ability to describe the adsorption process and determine the attainment of the saturation level.

3.11.2. Pseudo Second order kinetic study

With same concentrations of heavy metal ions used in the above studies was used in this kinetic model to estimate the development of heavy metal ions adsorption using activated biochar adsorbent. The kinetic plots (t/q vs. t) for this model is shown in Figure 8(d), (e) & (f) and Table 3 represents the constants of this kinetic model. The Pseudo second order constants were found to be in good agreement with the adsorption process and the calculated R^2 values are more than 0.95 was confirmed the applicability of kinetic study. By considering the suitability of both first-order and second-order kinetics, it can be concluded that the adsorption process of heavy metal ions in synthetic solutions reached a state of saturation (langeroodi et al, 2018).

3.11.3. Elovich kinetic model

In this study, Figure 9 (a), (b) and (c) were generated by plotting qt against ln(t) to assess the applicability of the Elovich kinetic model in the adsorption process of targeted metal ions (Cr, Ni, and Zn). However, the regression values obtained from this model were found to be low when compared to the second-order kinetic studies (as indicated in Table 3). The lower R^2 values obtained from the Elovich kinetic model suggest that it may not accurately fit the empirical evidence regarding the adsorption of targeted heavy metal ions using Gracilaria edulis as the adsorbent. Therefore, it appears that the assumption of a chemisorption process with a linear relationship between qt and ln(t) may not accurately describe the adsorption kinetics in this specific case. Based on the lower R^2 values obtained from the Elovich kinetic model in comparison to second order, it is recommended to prioritize the use of the pseudo-second-order model when studying the adsorption kinetics of metal ions onto Gracilaria edulis in this study. It is worth noting that the Elovich model is commonly employed to describe the kinetics of adsorption processes involving heterogeneous adsorbents (Momina et al, 2019). Despite having lower R^2 values compared to the pseudo-second-order model, the Elovich model can still provide valuable insights into the adsorption behavior on the heterogeneous surface of Gracilaria edulis.

3.11.4. Boyd kinetic model

Figure 9(d), (e) and (f) depict the graphs of Bt versus t, illustrating the elimination of targeted pollutants (Cr, Ni, and Zn) using Gracilaria edulis at different concentrations. These graphs exhibit a circular shape that does not intersect the origin. This observation indicates that intra-particle diffusion does not control the rate-determining step in the adsorption process. Bt versus t graphs are commonly utilized to assess the involvement of intra-particle diffusion in techniques for removing metal ions. Linear graphs passing through the origin suggest that intra-particle diffusion is the controlling factor in the adsorption process (Saavedra et al, 2018).

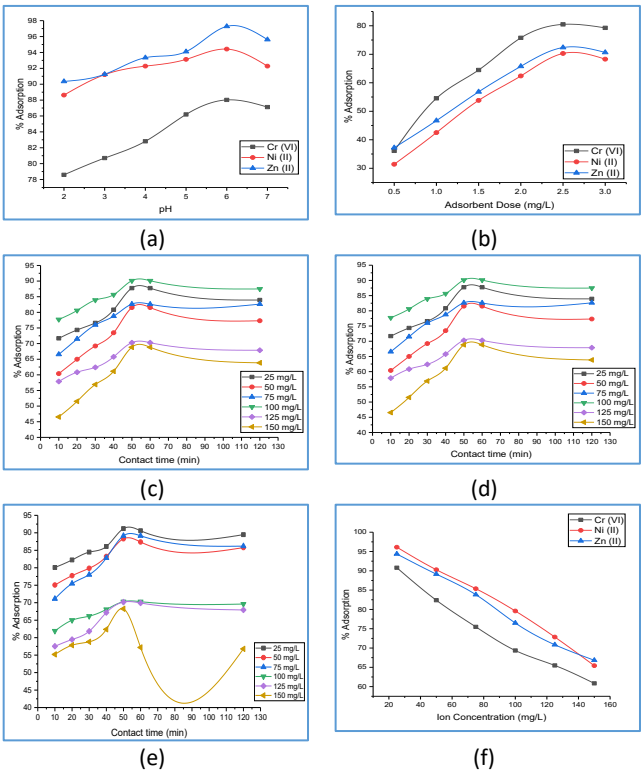

Figure 6. Changes in metal ion efficiency by adjusting (a) pH, (b) GE biochar dose, (c), (d) & (e) Contact time for Cr, Ni & Zn ions, (f) Concentrations of metal ions

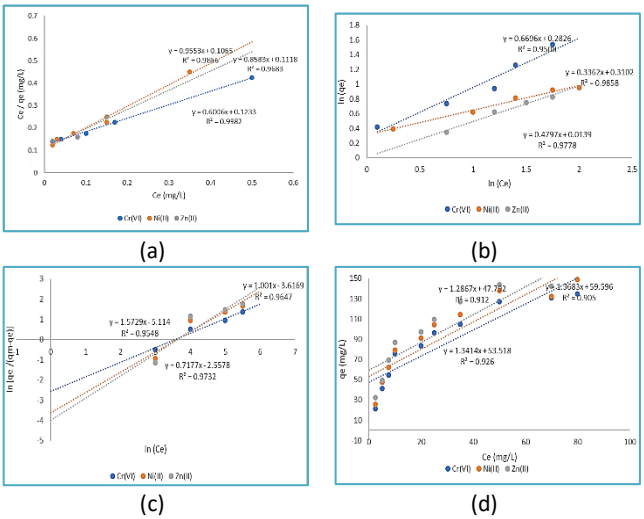

Figure 7. (a) Langmuir, (b) Freundlich, (c) Sips & (d) Toth – isotherm plots for the metal ion adsorption using GE biochar seaweed

Conversely, circular graphs that do not intersect the origin indicate that external or film diffusion is the primary mechanism inducing the metal ion adsorption. The diffusion coefficient (Di), intercept (B), and corresponding

regression coefficient (R^2) obtained from the Bt versus t graphs and it is represented in Table 3. Gracilaria edulis is able to adsorb metal ions onto a film of external diffusion, which is further supported by the regression and rate constant values.

Table 2. Constants of isothermal model for the adsorption of heavy metal ions using GE biochar seaweed

S. No.	Model	Parameters	Calculated values		
			Cr (VI)	Ni (II)	Zn (II)
1.	Langmuir	q_{max}	10.472	8.124	9.608
		K_L	0.436	0.385	0.510
		R^2	0.9982	0.9866	0.9683
2.	Freundlich	K_f	2.398	1.306	2.547
		n	3.102	2.823	3.049
		R^2	0.926	0.9858	0.9778
3.	Sips	K_S	11.869	10.735	12.263
		β_S	1.5823	2.0082	1.6730
		a_S	0.2316	0.2631	0.2225
		R^2	0.9548	0.9647	0.9732
4.	Toth	Q_{max}	26.983	25.473	24.800
		b_T	0.412	0.309	0.524
		n_T	0.690	0.737	0.610
		R^2	0.926	0.905	0.912

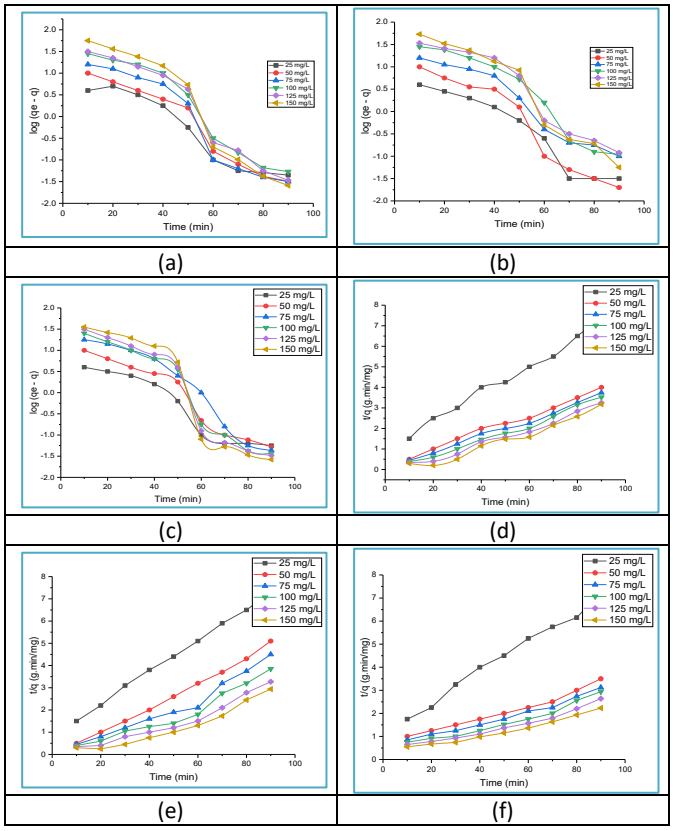

Figure 8. Pseudo plots for (a), (b) & (c) First order and (d), (e) & (f) – Second order of Cr, Ni& Zn metal ion adsorption using GE biochar

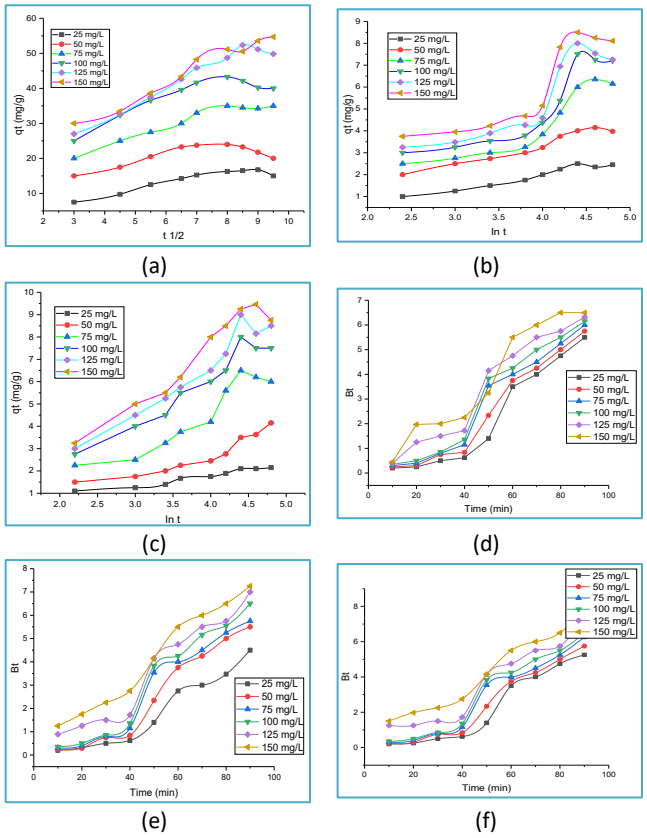

Figure 9. (a), (b) & (c) – Elovich and (d), (e) & (f) – Boyd - kinetic plots of Cr, Ni& Zn metal ion adsorption using GE biochar

Table 3. Kinetic constants for metal ions adsorption

S.No.	Type of metal	Conc. (mg/L)	Pseudo First order			Pseudo Second order				Elovich			Boyd		
			K (min^{-1})	q_e, cal (mg/g)	R^2	K (g/mg. min) X 10^{-3}	q_e, cal (mg/g)	h (mg/g.min)	R^2	a (mg/g. min)	b (g/mg)	R^2	B	D_i (X 10^{-3} m^2/s)	R^2
1.	Cr (VI)	25	0.034	2.64	0.95	16.69	2.15	0.10	0.96	0.244	1.55	0.94	0.034	5.472	0.915
2.		50	0.043	7.02	0.93	5.73	5.19	0.18	0.98	0.988	0.74	0.93	0.044	7.340	0.973
3.		75	0.041	10.00	0.93	3.34	8.30	0.22	0.98	0.978	0.55	0.92	0.043	7.621	0.963
4.		100	0.039	11.36	0.94	5.07	10.75	0.26	0.98	0.948	0.44	0.95	0.039	6.856	0.914
5.		125	0.048	17.47	0.92	2.00	12.91	0.29	0.97	0.977	0.35	0.92	0.049	8.725	0.982
6.		150	0.045	19.43	0.93	3.12	13.82	0.30	0.96	0.934	0.26	0.92	0.045	7.452	0.952
7.	Ni (II)	25	0.046	3.68	0.91	12.62	2.70	0.10	0.97	0.263	1.16	0.91	0.046	7.678	0.943
8.		50	0.041	6.54	0.93	5.32	5.47	0.12	0.98	0.328	0.81	0.94	0.041	6.294	0.983
9.		75	0.043	9.95	0.92	3.56	8.60	0.23	0.98	0.541	0.65	0.93	0.045	7.959	0.924
10.		100	0.046	12.38	0.94	2.77	10.10	0.28	0.97	0.611	0.47	0.92	0.046	7.678	0.983
11.		125	0.052	20.55	0.92	2.30	11.56	0.31	0.98	0.618	0.31	0.90	0.053	8.590	0.941
12.		150	0.050	25.48	0.94	2.65	12.73	0.33	0.96	0.596	0.20	0.92	0.055	8.972	0.922
13.	Zn (II)	25	0.039	2.84	0.95	15.43	2.14	0.09	0.96	0.230	1.63	0.94	0.037	6.428	0.993
14.		50	0.032	6.51	0.93	5.31	5.55	0.15	0.99	0.323	0.87	0.96	0.041	6.492	0.939
15.		75	0.041	10.40	0.91	3.64	7.74	0.21	0.97	0.484	0.65	0.94	0.046	7.687	0.920
16.		100	0.044	13.27	0.95	2.86	9.40	0.27	0.98	0.572	0.46	0.93	0.050	8.344	0.942
17.		125	0.044	18.35	0.94	1.35	12.64	0.23	0.98	0.652	0.36	0.92	0.049	8.725	0.941
18.		150	0.051	23.47	0.95	1.11	15.23	0.25	0.95	0.549	0.25	0.91	0.045	8.921	0.955

3.12. Thermodynamic and temperature studies

Under the optimum conditions by referring the batch studies, the studies were conducted by shifting the temperature of metal ion solution from 15° - 45°C and the effect of changes in metal ion adsorption has been investigated using GE biochar. The metal ion adsorption using GE biochar and its variations are shown in Figure 10 (a) (b) (c). There was an upward trend in heavy metal ions uptake when the temperature reaches 20°C and beyond that there is no change in heavy metal ions adsorption. When the temperature goes more than 20°C, a sudden drop in heavy metal ion adsorption was witnessed due to endothermic nature and decrease in the biochar adsorbent surface (Kalavathy et al, 2014). The thermodynamic plots of heavy metal ions adsorption process using biochar activated carbon adsorbent is exposed in Figure 10 (d) (e) (f) and Table 4 represents the slope and intercept (ΔH_o and ΔS_o) values of each plot. Also, ΔG_o values were determined to have negative values, along with positive ΔH_o values, indicating the spontaneous nature of activated biochar adsorbent material and its reaction to be endothermic (Indhumathi et al, 2014). The interaction between solid and liquid particles and its uncertainty was observed with positive ΔS_o values during the adsorption process.

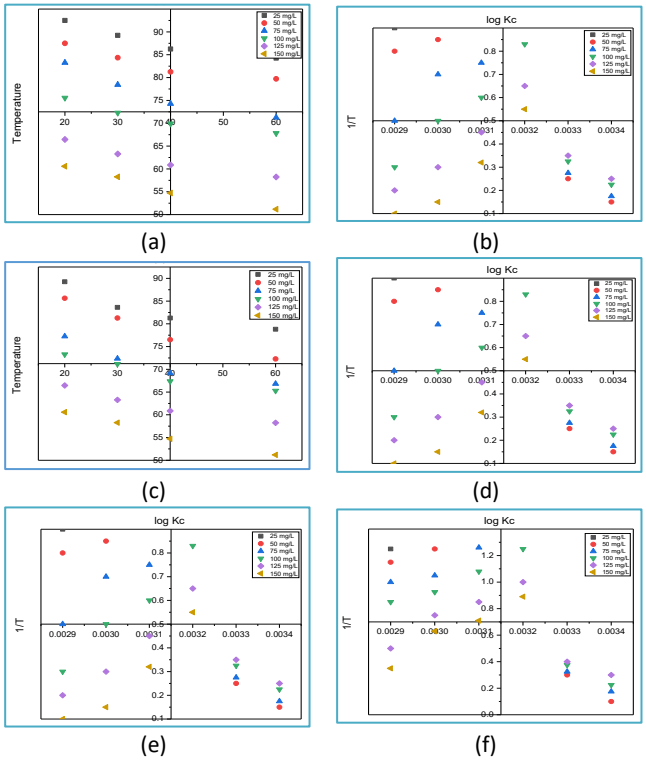

Figure 10. (a), (b) & (c) – Thermodynamic plots and (d), (e) & (f) – Temperature effect plots for targeted metal ions (Cr, Ni & Zn) adsorption using GE biochar seaweed

3.13. Desorption and regeneration studies

Recovery of adsorbed heavy metal ions and spent adsorbent is an important process in adsorption studies. Using concentrated hydrochloric acid with 0.1 N to 0.4 N, the heavy metal ions and biochar adsorbent material was recovered and amount of heavy metal ions desorbed by the HCl solution are listed in Table 5. The highest recovery of heavy metal ions was observed when 0.3N HCl acid was added and the concentration goes above 0.3 N, a sudden decrement was noticed. The recovery of heavy metal ions was reached to the constant rate when the concentration of HCl increased. As a result, the maximum amount of heavy metal ions was obtained by adding 0.3N HCl acid, which was then used for further experiments. On the other hand, the performance of batch adsorption process was evaluated by regeneration studies in three different cycles up to the saturation time. The optimum value of 0.3 N of HCl obtained from desorption studies, three different cycles were performed in regeneration process. After each adsorption cycle, the heavy metal ions were placed inside an oven at 140°F up to eight hours and reused. At the first stage of regeneration 89.27% of Cr, 82.81% of Ni and 84.37% of Zn heavy metal ions were recovered and used for regeneration process. With further increase in adsorption cycle, the rate of regeneration was reduced consistently. Therefore, the highest level of regeneration was attained during the initial cycle of the desorption process. Finally, the adsorbed materials were disposed through remote land filling method to avoid further creation of toxic effects to the surrounding environment.

4. Conclusion

Activated biochar Gracilaria edulis adsorbent used to remove heavy metal ions from aqueous solutions was carried out. The following are the findings obtained from the batch mode of studies. The highest level of adsorption of heavy metal ions from the aqueous solutions occurred at a pH of 2.0, using a GE biochar dose of 2 mg/L, a concentration of 25 mg/L for the heavy metal ions, and a contact time of 50 minutes. Throughout the batch adsorption studies, the solution temperature was kept at a steady 86°F. Models for Langmuir, Freundlich, and Sips isotherms show a favorable fit to the adsorption process. Also, the metal ion adsorption demonstrated excellent agreement with both Pseudo second-order and Elovich, as evidenced by high regression fits. The process of heavy metal adsorption for chromium (Cr), nickel (Ni), and zinc (Zn), using the activated carbon derived from Gracilaria edulis powder achieves 99.9%, 97.37%, and 92.73% removal rates, respectively. The most effective reclamation of metallic cations was accomplished by utilizing 0.3 N hydrochloric acid on the depleted adsorbent.

Table 4. Thermodynamic constants of heavy metal removal using GE biochar

Concentration of Cr (VI) metal ions (mg/L)	Entropy (ΔS°) KJ/mol	Enthalpy (ΔH°) J/mol	Gibbs Energy (ΔGo) kJ/mol			
			15°C	30°C	45°C	60°C
25	83.482	189.320	-14.293	-10.042	-9.025	-7.203
50	41.294	99.042	-10.452	-8.204	-7.239	-5.928
75	25.493	49.023	-8.296	-7.204	-6.245	-5.293
100	16.395	33.842	-5.395	-5.121	-4.921	-4.548
125	12.041	29.456	-3.534	-3.252	-3.576	-3.201
150	8.945	25.923	-2.042	-1.943	-1.843	-1.652
Concentration of Ni (II) metal ions (mg/L)						
25	73.945	163.494	-12.943	-10.943	-8.239	-7.543
50	39.298	83.723	-10.284	-9.204	-7.283	-5.892
75	24.035	40.294	-8.593	-8.023	-6.032	-4.925
100	18.204	21.049	-6.402	-5.394	-4.785	-3.024
125	13.543	16.305	-4.203	-3.253	-3.012	-2.435
150	9.836	10.423	-3.021	-2.893	-2.324	-1.936
Concentration of Zn (II) metal ions (mg/L)						
25	78.239	174.293	-10.384	-8.694	-6.943	-5.354
50	35.204	84.394	-8.845	-6.485	-5.403	-4.832
75	18.294	43.293	-7.034	-5.832	-4.235	-3.548
100	12.042	22.394	-5.934	-4.674	-3.293	-2.854
125	9.920	12.391	-4.353	-3.240	-2.594	-2.031
150	7.239	8.492	-3.065	-2.863	-1.865	-1.429

Table 5. Desorption of heavy metal ions from the activated biochar *Gracilaria edulis*

Concentration of metal ions (25 mg/L)	Recovery of heavy metal ions (%)	Normality of Sulfuric Acid			
		0.10 N	0.20 N	0.30 N	0.40 N
		Desorption rate of targeted metal ions in %			
Cr (VI)	99.32	90.48	92.31	95.42	92.05
Ni (II)	91.28	82.63	85.72	87.95	83.52
Zn (II)	87.37	79.92	82.37	84.18	81.35

References

Alardhi S.M., Albayati T.M. and Alrubay J.M. (2020). Adsorption of the methyl green dye pollutant from aqueous solution using mesoporous materials MCM-41 in a fixed-bed column, *Heliyon*, **6** (1), e03253.

Benjelloun M., Miyah Y., Evrendilek G.A., Lairini F.Z.S. (2021). Recent Advances in Adsorption Kinetic Models: Their Application to Dye Types, *Arabian Journal of Chemistry*, **14** (4), 103031.

Boubaker H., Arfi R.B., Mougin K., Vaulot C., Hajj S., Kunneman P., Schrodj G. and Ghorbal A. (2021). New optimization approach for successive cationic and anionic dyes uptake using reed-based beads, *Journal of Cleaner Production*, **307**, 127218.

Chakraborty R., Asthana A., Singh A.K., Jain B.and Susan A.B.H. (2022). Adsorption of heavy metal ions by various low-cost adsorbents: a review, *International Journal of Environmental Analytical Chemistry*, **102** (2), 342–349.

Eleryan A., Aigbe U.O., Ukhurebor K.E., Onyancha R.B., Eldeeb T.M., El-Nemr M.A., Hassaan M.A., Ragab S., Osibote O.A., Kusuma H.S., Darmokoesoemo H. and El Nemr A. (2022). Copper(II) ion removal by chemically and physically modified sawdust biochar, *Biomass Conversion and Biorefinery*.

Eleryan A., Aigbe U.O., Ukhurebor K.E., Onyancha R.B., Eldeeb T.M. , El-Nemr M.A., Hassaan M.A., Ragab S., Osibote O.A., Kusuma H.S., Darmokoesoemo H. and El Nemr A. (2022). Copper(II) ion removal by chemically and physically modified sawdust biochar. *Biomass Conversion and Biorefinery*.

Fakhar N., Khan S.A., Siddiqi W.A. and Khan T.A. (2021). Ziziphus jujube waste-derived biomass as cost-effective adsorbent for the sequestration of Cd2+ from aqueous solution: Isotherm and kinetics studies. Environmental Nanotechnology, *Monitoring & Management*, **16**, 100570.

Fideles R.A., Teodoro F.S., Xavier A.L.P, Adarme O.F.H., Gil L.F. and L.V.A. (2019). Trimellitated sugarcane bagasse: A versatile adsorbent for removal of cationic dyes from aqueous solution. Part II: Batch and continuous adsorption in a bicomponent system, J*ournal of Colloid and Interface Science*, **552** (15), 752–763.

Gómez-Aguilar D.L., Rodríguez-Miranda J.P. and Salcedo-Parra O.J. (2022). Fruit Peels as a Sustainable Waste for the Biosorption of Heavy Metals in Wastewater: A Review, *Molecules*, **27**, 2124.

Haro N.K., Dávila I.V.J., Nunes K.G.P., de Franco M.A.E., Marcilio N.R. and Féris L.A. (2021). Kinetic, equilibrium and thermodynamic studies of the adsorption of paracetamol in activated carbon in batch model and fixed-bed column, **11** (38).

Indhumathi P., Shabudeen P.S.S., Shoba U.S. and Saraswathy C.P., The removal of chromium from aqueous solution by using green micro algae, *Journal of Chemical and Pharmaceutical Research*, **6** (2014) 799–808.

Isam M., Baloo L. and Chabuk A. (2023). Optimization and modelling of Pb (II) and Cu (II) adsorption onto red algae (Gracilaria changii)-based activated carbon by using response surface methodology, *Biomass Conversion and Biorefinary.*

Kalavathy M.H., Karthikeyan T., Rajgopal S., Miranda L.R., Kinetic and isotherm studies of Cu (II) adsorption onto HPO-activated rubber wood sawdust, *Journal of Colloidal Interface Sciences*, **292** (2014) 354–362.

Kaminski W., Tomczak E. and Tosik P. (2015). Kinetics of azo dyes sorption onto low-cost sorbents, Desalination and Water *Treatment*, **55**, 2675–2679.

Khan N., Wahid F., Sultana Q., Us Saqib N. and Rahim M. (2020). Surface oxidized and un-oxidized activated carbon derived from Ziziphus jujube Stem, and its application in removal of Cd (II) and Pb (II) from aqueous media. *SN Applied Sciences*, **2**, 753.

Khan T.A., Noumana Md., Dua D., Khan S.A. and Alharthi S.S. (2022). Adsorptive scavenging of cationic dyes from aquatic phase by H3PO4 activated Indian jujube (Ziziphus mauritiana) seeds based activated carbon: Isotherm, kinetics, and thermodynamic study, *Journal of Saudi Chemical Society*, **26** (2), 101417.

Konicki W., Aleksandrzak M., Moszyński D. and Mijowska E. (2017). Adsorption of anionic azo-dyes from aqueous solutions onto graphene oxide: Equilibrium, kinetic and thermodynamic studies, *Journal of Colloid and Interface Science*, **496**, 188–200.

Langeroodi N.S., Farhadravesh Z. and Aliakbar dehno khalaji. (2018). Optimization of adsorption parameters for Fe (III) ions removal from aqueous solutions by transition metal oxide nanocomposite, *Green chemistry letters and reviews*, **11** (4), 404–413.

Marciniak M., Goscianska J., Norman M., Bazan-Wozniak T.J.A. and Pietrzak R. (2022). Equilibrium, Kinetic, and Thermodynamic Studies on Adsorption of Rhodamine B from Aqueous Solutions Using Oxidized Mesoporous Carbons, *Materials*, **15**, 5773.

Momina, Rafatullah M., Ismail S. and Ahmed A. (2019). Optimization Study for the Desorption of Methylene Blue Dye from Clay Based Adsorbent Coating, *Water*, **11**, 1304.

Murthy T.P.K. and Gowrishankar B.S. (2020). Process optimization of methylene blue sequestration onto physical and chemical treated coffee husk-based adsorbent, *SN Applied Sciences*, **2**, 836.

Nippes R.P., Macruz P.D., Molina L.C.A. and Scaliante M.H.N.O. (2022). Hydroxychloroquine Adsorption in Aqueous Medium Using Clinoptilolite Zeolite, Water, Air, & Soil Pollution, **233**, 287.

Obulapuram P.K., Arfin T., Mohammad F., Khiste S.K., Chavali M., Albalawi A.N. and Al-Lohedan H.A. (2021). Adsorption, Equilibrium Isotherm, and Thermodynamic Studies towards the Removal of Reactive Orange 16 Dye Using Cu(I)-Polyaninile Composite, *Polymers*, **13** (20), 3490.

Pham B.N., Kang J.K., Lee C.G. and Park S.J. (2021). Removal of Heavy Metals (Cd2+, Cu2+, Ni2+, Pb2+) from Aqueous Solution Using Hizikia fusiformis as an Algae-Based Bioadsorbent, *Applied Sciences*, **11** (18), 8604.

Priya A.K., Yogeshwaran V., Rajendran S., Hoang T.K.A., Soto-Moscoso M., Ghfar A.A. and Bathula C. (2022). Investigation of mechanism of heavy metals (Cr^{6+}, Pb_{2+}& Zn^{2+}) adsorption from aqueous medium using rice husk ash: Kinetic and thermodynamic approach, *Chemosphere*, **286**, 131796.

Saavedra R., Muñoz R., Taboada M.E., Vega M. and Bolado S. (2018). Comparative uptake study of arsenic, boron, copper, manganese and zinc from water by different green microalgae, *Bioresource Technology*, **263**, 49–57.

Sheeja J., Sampath K. and Kesavasamy R. (2021). Experimental Investigations on Adsorption of Reactive Toxic Dyes Using

Hedyotis umbellate Activated Carbon, *Adsorption Science and Technology*, ID–5035539.

Singh J., Dhiman N. and Sharma N.K. (2018). Effect of Fe(II) on the Adsorption of Mn(II) from Aqueous Solution Using Esterified Saw Dust: Equilibrium and Thermodynamic Studies, *Indian Chemical Engineer*, **60** (3), 255–268.

Su L., Zhang H., Oh K., Liu N., Luo Y., Cheng H., Zhang G. and He X. (2021). Activated biochar derived from spent Auricularia auricula substrate for the efficient adsorption of cationic azo dyes from single and binary adsorptive systems, *Water Science & Technology*, **84** (1), 101–121.

Venkataraghavan R., Thiruchelvi R. and Sharmila D. (2020). Statistical optimization of textile dye effluent adsorption by Gracilaria edulis using Plackett-Burman design and response surface methodology, *Heliyon*, **6** (10) , e05219.

Venkatraman Y. and Priya A.K. (2021). Removal of heavy metal ion concentrations from the wastewater using tobacco leaves coated with iron oxide nanoparticles, International *Journal of Environmental Science and Technology*, **19**, 2721–2736.

Wang C., Wang X., Li N., Tao J., Yan B., Cui X., Chen G., Adsorption of Lead from Aqueous Solution by Biochar: A *Review. Clean Technologies*, **4** (2022), 629–652.

Xi L., Zhou S., Zhang C., Fu Z., Wang A., Zhang Q., Wang Y., Liu X., Wang X. and Xua W. (2020). Environment-friendly Juncus effusus-based adsorbent with a three-dimensional network structure for highly efficient removal of dyes from wastewater, *Journal of Cleaner Production*, **259**, 120812.

Yan C. Z., Kim M. G., Hwang H. U., Nzioka A. M., Sim Y. J. and. Kim Y. J. (2020). Adsorption of Heavy Metals Using Activated Carbon Synthesized from the Residues of Medicinal Herbs, *Theoretical Foundations of Chemical Engineering*, 54, 973–982.

Yogeshwaran V. and Priya A.K. (2021). Experimental studies on the removal of heavy metal ion concentration using sugarcane bagasse in batch adsorption process. *Desalination and Water Treatment*, **224**, 256–272.